



Published in final edited form as:

Science. 2008 March 7; 319(5868): 1405–1408.

## Coiled-Coil Irregularities and Instabilities in Group A *Streptococcus* M1 Are Required for Virulence

Case McNamara<sup>1,\*</sup>, Annelies S. Zinkernagel<sup>2</sup>, Pauline Macheboeuf<sup>1</sup>, Madeleine W. Cunningham<sup>3</sup>, Victor Nizet<sup>2,4</sup>, and Partho Ghosh<sup>1,5,†</sup>

<sup>1</sup>Department of Chemistry and Biochemistry, University of California, San Diego, La Jolla, CA 92093, USA

<sup>2</sup>Department of Pediatrics, University of California, San Diego, La Jolla, CA 92093, USA

<sup>3</sup>University of Oklahoma Health Sciences Center, Biomedical Research Center, 975 North East 10th Street, Oklahoma City, OK 73104, USA

<sup>4</sup>School of Pharmacy and Pharmaceutical Sciences, University of California, San Diego, La Jolla, CA 92093, USA

<sup>5</sup>Section of Molecular Biology, University of California, San Diego, La Jolla, CA 92093, USA

### Abstract

Antigenically variable M proteins are major virulence factors and immunogens of the human pathogen group A *Streptococcus* (GAS). Here, we report the ~3 angstrom resolution structure of a GAS M1 fragment containing the regions responsible for eliciting type-specific, protective immunity and for binding fibrinogen, which promotes M1 proinflammatory and antiphagocytic functions. The structure revealed substantial irregularities and instabilities throughout the coiled coil of the M1 fragment. Similar structural irregularities occur in myosin and tropomyosin, explaining the patterns of cross-reactivity seen in autoimmune sequelae of GAS infection. Sequence idealization of a large segment of the M1 coiled coil enhanced stability but diminished fibrinogen binding, proinflammatory effects, and antibody cross-reactivity, whereas it left protective immunogenicity undiminished. Idealized M proteins appear to have promise as vaccine immunogens.

M proteins are major virulence factors of group A *Streptococcus* (GAS), a bacterial pathogen responsible for mild-to-life-threatening diseases against which no vaccines currently exist (1). Fibrils of ~500 Å-long M protein form a dense, covalently attached coat on the streptococcal surface (2,3). Host proteins, such as fibrinogen (4), bind specifically to M proteins and block deposition of opsonic antibodies and complement, preventing phagocytic elimination of GAS by neutrophils (1,5). A clone expressing the M1 antigenic variant of M protein emerged nearly three decades ago and has persisted as the leading cause of severe invasive GAS infection (6). Intact M1 and M1 fragments released by neutrophil proteases are sufficient to evoke pulmonary hemorrhage, inflammation, and tissue destruction that is characteristic of severe infection (7). These effects depend on M1 binding to fibrinogen, which triggers release of heparin binding protein (HBP), a mediator of vascular leakage, from neutrophils (7).

M proteins are also prominently associated with autoimmune sequelae of GAS infection, such as rheumatic fever, which is problematic for vaccine development (8) and remains a serious threat in the developing world. In rheumatic fever patients, potentially immunogenic M proteins elicit cross-reactive antibodies and T cell receptors directed against host  $\alpha$ -helical coiled-coil

†To whom correspondence should be addressed. E-mail: pghosh@ucsd.edu.

\*Present address: Genomics Institute of the Novartis Research Foundation, 10675 John Jay Hopkins Drive, San Diego, CA 92121, USA.

proteins, such as myosin and tropomyosin (1). Cross-reactivity is probably attributable to molecular mimicry, as M proteins appear to form coiled coils as well (2,3,9,10). As with myosin and tropomyosin, M proteins contain coiled-coil destabilizing sequences (11–13)—that is, insertions within heptads and charged residues and Ala residues at *a* and *d* heptad positions (Fig. 1).

To understand the effects of such unusual sequence features in M proteins, we crystallized a fragment of M1 (called M1<sup>AB</sup>, residues 42 to 194) (14). The M1<sup>AB</sup> fragment contains the A region, whose first 50 residues, known as the hypervariable region (HVR), elicit type-specific, protective antibodies (5) and are part of a promising multivalent vaccine in clinical trials (15). The fragment also contains the B repeats, which are implicated in fibrinogen binding (4) and were sufficient to bind fibrinogen fragment D (FgD) (16) (fig. S1). M1<sup>AB</sup> is similar to a proinflammatory fragment generated by neutrophil proteases (7).

The 3.04 Å resolution structure of M1<sup>AB</sup> revealed that, whereas most of the A region formed a dimeric, parallel coiled coil, the B repeats had splayed apart and intertwined with the B repeats of adjacent M1<sup>AB</sup> molecules via antiparallel coiled coils (Fig. 1C, fig. S2, and table S1). The antiparallel association was probably an artifact of crystallization but is suggestive of instabilities in the B repeats.

Except for two short stretches of ideal parallel coiled coil (residues 63 to 79 and 106 to 119), the structure of M1<sup>AB</sup> was irregular throughout its ~200 Å length (Fig. 2A). The first of four major irregularities was an Ala stagger in the HVR. Poor packing of three Ala residues clustered at *a* and *d* positions led to local deformities; that is, a tightening of the coiled-coil radius from 5.0 to 4.25 Å, a ~2.5 Å asymmetric staggering of opposing helices, and a flexible hinge (Fig. 2, B and C, and fig. S3). Similar staggers and bends occur in tropomyosin (17,18) and cardiac myosin (19) and are suggested to provide flexibility for function.

The second form of irregularity was super-helical unwinding due to Lys<sup>98</sup> and Arg<sup>105</sup> at successive *a* positions. These residues faced away from the coiled-coil core and contacted solvent-exposed residues (Fig. 2D), resulting in a loosening of the coiled-coil pitch from 150 Å to ~200 to 225 Å and an expansion of the coiled-coil radius to 5.4 Å (fig. S3). Unwinding resulting from Lys and Arg residues at *a* positions has been implicated in myosin function (19,20) and also occurs in tropomyosin (17).

The third irregularity was attributable to an extra residue in the first heptad of the B repeats (Fig. 1B). The destabilizing effect of eight residues in a heptad (13) was accommodated by a +1 frameshift in the heptad register, precluding continuation of the parallel coiled coil. The fourth irregularity followed with the splaying apart of the B repeats and the formation of antiparallel coiled coils. The antiparallel orientation, with its *a-d'* (prime refers to the opposing helix) core packing (Fig. 2E), was probably preferable to the parallel orientation with its *a-a'* charge-charge clashes and *d-d'* Ala-Ala packing. Splaying at the ends of myosin (19) and tropomyosin (21,22) coiled coils also occurs and is implicated in function.

Consistent with the prevalence of structural irregularities in M1<sup>AB</sup>, the circular dichroism (CD) spectrum of this fragment at 37°C showed a marked loss in  $\alpha$ -helical content and a 222:208 nm ratio < 1 (Fig. 3A). Because this ratio is  $\geq 1$  for coiled coils and  $\leq 0.86$  for isolated helices (23), these data suggested that M1<sup>AB</sup> exchanges between monomer and dimer states. This conclusion was supported by static light-scattering measurements, which provided evidence for the coexistence of M1<sup>AB</sup> monomers and dimers (fig. S4).

Intact M1 (residues 42 to 453) showed a comparable loss of  $\alpha$ -helical content at 37°C (Fig. 3B) (10). To determine whether monomer/dimer exchange also occurred in intact M1, we incubated His<sub>6</sub>-tagged M1 dimers (M1-H/M1-H) with untagged M1 dimers (M1/M1).

Dissociation and exchange producing M1-H/M1 heterodimers was evident at 37°C but not at lower temperatures (Fig. 3C). Similarly, dissociation of M1-H/M1 heterodimers occurred at 37°C but not at lower temperatures (Fig. 3C). These results indicated that structural instabilities in M1, although dampened at low temperatures, are prominent at physiological temperature.

To investigate the role of structural instability in M1, we focused on the B repeats, owing to their sufficiency for fibrinogen binding. Thirteen substitutions were introduced to set *a* and *d* positions in the B repeats to Val and Leu, respectively, yielding M1\* (residues 42 to 453) and M1<sup>AB\*</sup> (residues 42 to 194) (Fig. 1B and fig. S5A). These substitutions made the core residues optimal for the formation of dimeric parallel coiled coils (12,24). In addition, we deleted Leu<sup>133</sup> from M1\* and M1<sup>AB\*</sup> [yielding M1\*( $\Delta$ L133) and M1<sup>AB\*</sup>( $\Delta$ L133), respectively] to remove the frameshift in the B repeats (fig. S5B).

All mutant proteins contained greater  $\alpha$ -helical content as compared with wild-type (WT) proteins at 37°C (Fig. 3). Although enhanced in stability, both M1\* and M1\*( $\Delta$ L133) bound significantly less FgD than did WT M1 at 37°C (Fig. 4, A and B). Binding to human immunoglobulin Gs, an interaction dependent on M1 regions outside the B repeats, was unaffected (fig. S6). Consistent with these results, human neutrophils stimulated with M1\*( $\Delta$ L133) released substantially less HBP as compared with M1 (Fig. 4C). Furthermore, when M1 was injected intravenously into mice, intra-alveolar edema was evident by 30 min in lung histopathologies of 4 out of 4 animals (Fig. 4D), but vascular leakage was absent in all mice injected with M1\*( $\Delta$ L133). M1\*( $\Delta$ L133) did retain some proinflammatory activity, as vascular congestion was comparable for M1 and M1\*( $\Delta$ L133).

We next examined the cross-reactivity of idealized M1 using an extensively characterized group of cross-reactive monoclonal antibodies (mAbs) (25). In this group, mAb 36.2.2, which recognizes myosin and tropomyosin and is also highly cytotoxic against heart cells (26), bound M1 most strongly but was 8 to 16 times less reactive against M1\* and M1\*( $\Delta$ L133) (Fig. 5A, fig. S7, and table S2). Thus, sequence idealization of M1 could reduce cross-reactivity.

Mice were then immunized with M1 or M1\*( $\Delta$ L133) and challenged with a WT strain of M1 GAS. M1 and M1\*( $\Delta$ L133) elicited similar titers of M1-reactive antibodies (fig. S8), and each afforded similar levels of protection against the development of skin lesions after subcutaneous GAS challenge (Fig. 5B). Similarly, M1 and M1\*( $\Delta$ L133) provided comparable levels of protection against acute bacteremia and mortality after intraperitoneal GAS challenge (Fig. 5, C and D).

Our results show that the specific structure of M1 causes proinflammatory interactions with fibrinogen. A comparable set of structural features occurs in myosin and tropomyosin (17–22), indicating a deep level of molecular similarity between M1 and these host proteins and explaining the patterns of cross-reactivity seen in rheumatic fever. Mutation to stabilize the structure of the M1 coiled coil reduced fibrinogen binding, proinflammatory effects, and recognition by a cross-reactive and cytotoxic antibody, whereas it left the immunogenic and protective properties of M1 undiminished.

## Supplementary Material

Refer to Web version on PubMed Central for supplementary material.

## References and Notes

1. Cunningham MW. Clin Microbiol Rev 2000;13:470. [PubMed: 10885988]
2. Fischetti VA. Clin Microbiol Rev 1989;2:285. [PubMed: 2670192]

3. Phillips GN Jr, Flicker PF, Cohen C, Manjula BN, Fischetti VA. *Proc Natl Acad Sci U S A* 1981;78:4689. [PubMed: 7029524]
4. Ringdahl U, et al. *Mol Microbiol* 2000;37:1318. [PubMed: 10998165]
5. Sandin C, Carlsson F, Lindahl G. *Mol Microbiol* 2006;59:20. [PubMed: 16359315]
6. Chatellier S, et al. *Infect Immun* 2000;68:3523. [PubMed: 10816507]
7. Herwald H, et al. *Cell* 2004;116:367. [PubMed: 15016372]
8. Massell BF, Honikman LH, Amezcua J. *JAMA* 1969;207:1115. [PubMed: 5818242]
9. Andre I, et al. *Biochemistry* 2006;45:4559. [PubMed: 16584191]
10. Nilson BH, et al. *Biochemistry* 1995;34:13688. [PubMed: 7577960]
11. Tripet B, Wagschal K, Lavigne P, Mant CT, Hodges RS. *J Mol Biol* 2000;300:377. [PubMed: 10873472]
12. Harbury PB, Kim PS, Alber T. *Nature* 1994;371:80. [PubMed: 8072533]
13. Hicks MR, Walshaw J, Woolfson DN. *J Struct Biol* 2002;137:73. [PubMed: 12064935]
14. Materials and methods are available as supporting material on *Science* Online.
15. McNeil SA, et al. *Clin Infect Dis* 2005;41:1114. [PubMed: 16163629]
16. Spraggon G, Everse SJ, Doolittle RF. *Nature* 1997;389:455. [PubMed: 9333233]
17. Brown JH, et al. *Proc Natl Acad Sci U S A* 2001;98:8496. [PubMed: 11438684]
18. Brown JH, et al. *Proc Natl Acad Sci U S A* 2005;102:18878. [PubMed: 16365313]
19. Blankenfeldt W, Thoma NH, Wray JS, Gautel M, Schlichting I. *Proc Natl Acad Sci U S A* 2006;103:17713. [PubMed: 17095604]
20. Li Y, et al. *Nature* 2003;424:341. [PubMed: 12867988]
21. Li Y, et al. *Proc Natl Acad Sci U S A* 2002;99:7378. [PubMed: 12032291]
22. Greenfield NJ, et al. *J Mol Biol* 2006;364:80. [PubMed: 16999976]
23. Lau SY, Taneja AK, Hodges RS. *J Biol Chem* 1984;259:13253. [PubMed: 6490655]
24. Kwok SC, Hodges RS. *J Biol Chem* 2004;279:21576. [PubMed: 15020585]
25. Mertens NM, Galvin JE, Adderson EE, Cunningham MW. *Mol Immunol* 2000;37:901. [PubMed: 11282394]
26. Cunningham MW, et al. *Proc Natl Acad Sci U S A* 1992;89:1320. [PubMed: 1311095]
27. This work was supported by NIH grant T32 GM008326 (C.M.), Swiss National Science Foundation fellowship PBZHB-108365 (A.S.Z.), NIH grant R01 AI048694 (V.N.), and American Heart Association and NIH grant R21 AI071167 (P.G.). We thank R. Doolittle, L. Pandi, S. Choe, S. Pegan, G. Allendorph, W. Blankenfeldt, S. Strelkov, G. Ghosh lab members, the staffs of Advanced Light Source 5.0.2 and Advanced Photon Source ID-19, N. Varki, A. Mascaro-Blanco, and S. Mel for reagents, expert technical assistance, or both. Coordinates and structure factors have been deposited in the Protein Data Bank ([www.rcsb.org](http://www.rcsb.org)) with the accession number 2OTO.

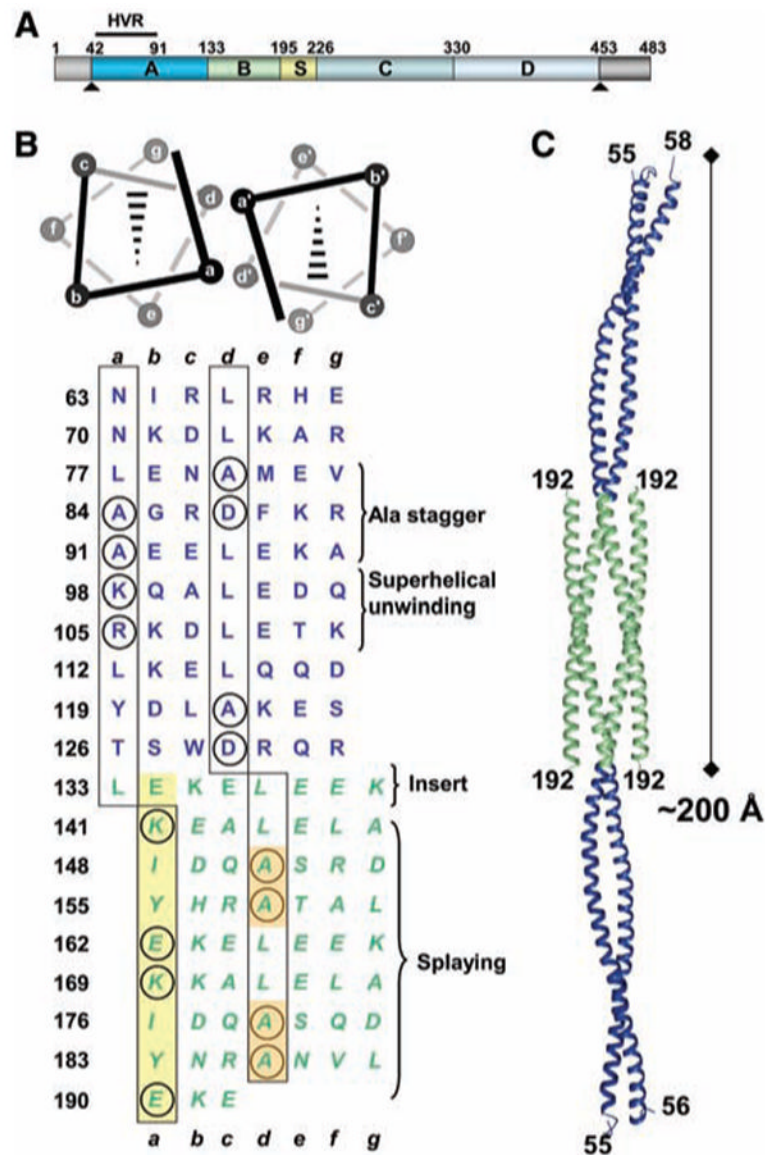


**Fig. 1.** (A) Mature M1 results from cleavage (arrowheads) of the N-terminal signal sequence and the C-terminal Leu-Pro-X-Thr-Gly motif (where X is any amino acid) and covalent attachment of the C terminus to the cell wall. Boundaries of the A region, B repeats, S region, C repeats, and D region are indicated. (B) (Top) *a-a'* and *d-d'* (prime refers to the opposing helix) packing in parallel dimeric coiled coils. Broken wedges indicate helices pointing the N to C termini into the page. (Bottom) Heptad register indicated above and below the sequence (*a* and *d* position residues boxed) of the M1 A region (blue) and B repeats (green). The circled residues are destabilizing to coiled coils, with relative instabilities  $\Delta\Delta G_u(\text{Ala}) \leq 0$  (11). Italicized residues form antiparallel coiled coils in the crystal. Residues highlighted in yellow and orange were substituted with Val and Leu, respectively, to create M1\* and M1<sup>AB\*</sup>. (C) Tail-to-tail packing of the two M1<sup>AB</sup> dimers in the asymmetric unit of the crystal (blue, A regions; green, B repeats).



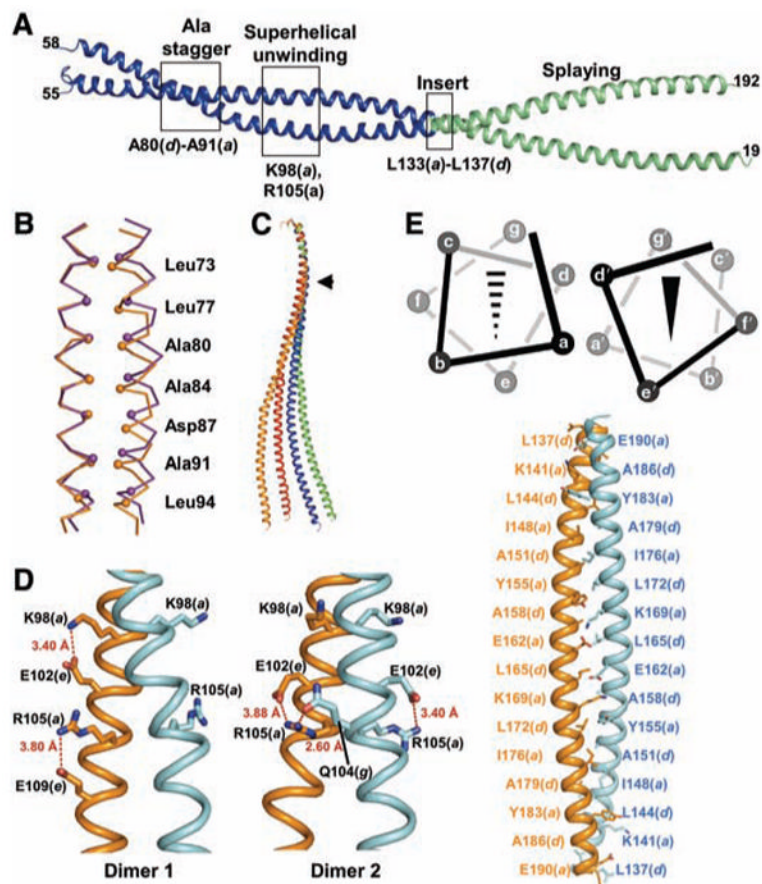


**Fig. 2.**  
 (A) Structure of M1<sup>AB</sup> (blue, A region; green, B repeats) with boxed regions and labeling indicating irregularities. (B) Ala stagger shown by superposition of C $\alpha$  traces of M1<sup>AB</sup> residues 70 to 97 (orange) with the ideal coiled coil of GCN4 (purple). (C) Conformation of individual helices from the two M1<sup>AB</sup> dimers in the asymmetric unit, superimposed on main-chain atoms of residues 60 to 77. The position of the Ala stagger is indicated by the arrowhead. (D) Conformation of Lys<sup>98</sup> and Arg<sup>105</sup> in the two M1<sup>AB</sup> dimers in the asymmetric unit, with heptad positions of residues indicated in parentheses and polar contacts in red dashed lines (with distances shown). (E) (Top) Schematic of *a-d'* and *d-a'* packing in antiparallel dimeric coiled coils. The broken wedge indicates the helix pointing the N to C termini into the page, and the solid wedge denotes out of the page. (Bottom) Antiparallel coiled coil of B repeats, with side chains of *a* and *d* position residues depicted and labeled.

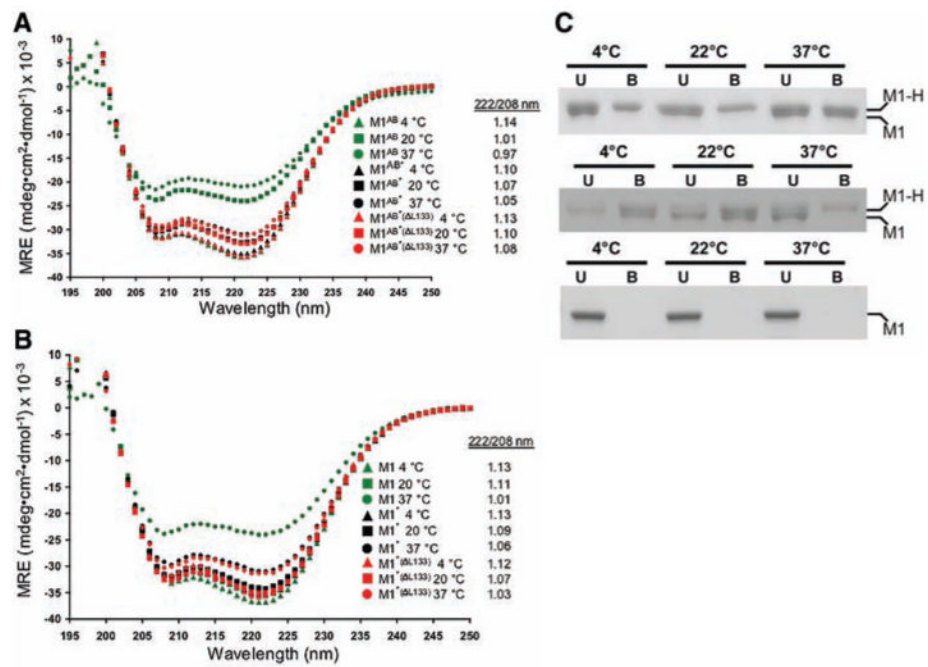


**Fig. 3.** CD spectra at 4 (triangles), 20 (squares), and 37°C (circles) of (A) M1<sup>AB</sup> (green), M1<sup>AB\*</sup> (black), and M1<sup>AB\*(ΔL133)</sup> (red) and (B) M1 (green), M1\* (black), and M1\*(ΔL133) (red). Mean residue 222:208 ellipticity (MRE) ratios are shown. (C) (Top) His<sub>6</sub>-tagged M1 (M1-H) and untagged M1 (M1) were coinubated at the indicated temperatures and coprecipitated at 4°C with Ni<sup>2+</sup>- nitrilotriacetic acid (NTA) agarose beads. (Middle) M1-H/M1 heterodimers were isolated, incubated, and coprecipitated at the indicated temperatures with Ni<sup>2+</sup>-NTA agarose beads. (Bottom) Only untagged M1 was incubated with beads. (A to C) Unbound protein (U) and protein bound to the beads (B) were visualized by Coomassie-stained, reducing SDS-polyacrylamide gel electrophoresis (PAGE).

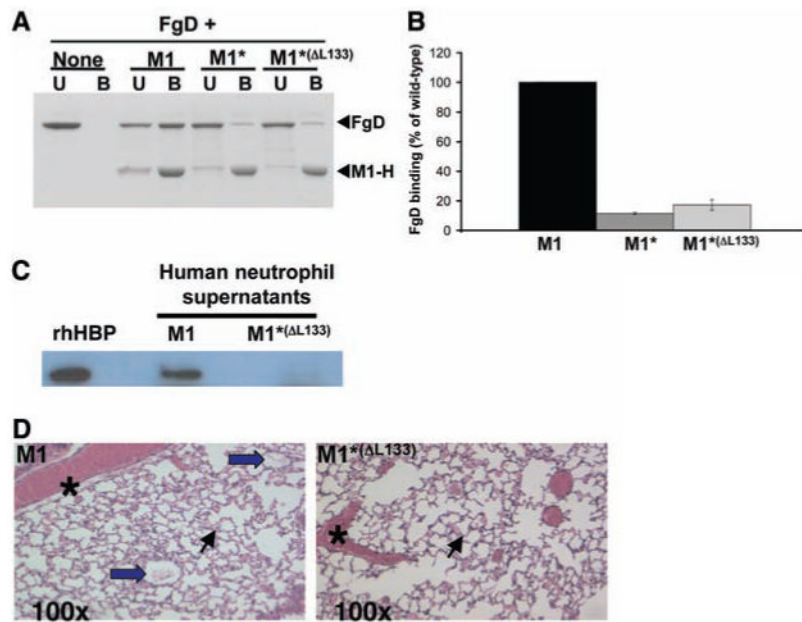


**Fig. 4.** (A) FgD incubated alone or with His<sub>6</sub>-tagged constructs of M1, M1\*, or M1\*( $\Delta$ L133) at 37°C and coprecipitated with Ni<sup>2+</sup>-NTA agarose beads. U and B proteins were visualized by Coomassie-stained, nonreducing SDS-PAGE. (B) Quantification of FgD binding in (A). Error bars indicate mean  $\pm$  SD. (C) Western blot of HBP in supernatants from human neutrophils stimulated with M1 or M1\*( $\Delta$ L133), rhHBP, recombinant human HBP. (D) Lung histopathology of Balb/c mice 30 min after intravenous injection of M1 or M1\*( $\Delta$ L133). Representative histopathology (hematoxylin and eosin stain) with intra-alveolar edema (thick blue arrows) and macrovascular (asterisks) and microvascular (thin arrows) congestion is indicated. Magnification,  $\times$ 100.



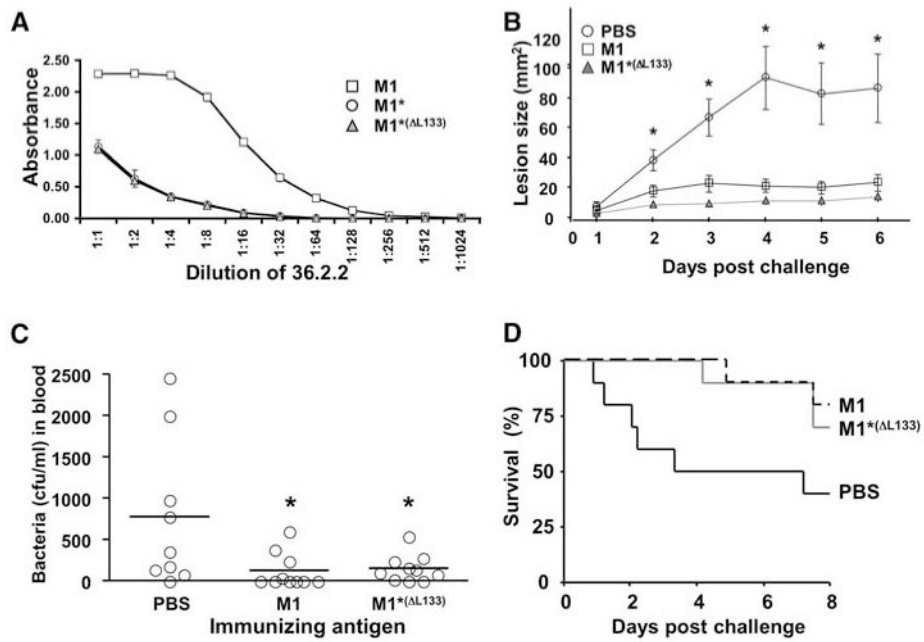


**Fig. 5.** (A) Titer of mAb 36.2.2 versus M1, M1\*, and M1\*( $\Delta$ L133) by enzyme-linked immunosorbent assay. Error bars indicate mean  $\pm$  SD. (B) Skin lesion size of mice immunized with M1 or M1\*( $\Delta$ L133) after subcutaneous challenge with WT M1 GAS. Error bars indicate mean  $\pm$  SEM ( $N = 10$  mice per group). Analysis of variance (ANOVA) was significant ( $P < 0.002$ ) on days 2 to 6; posthoc group comparisons (Tukey-Kramer multiple-comparison test) revealed significant protection of M1 or M1\*( $\Delta$ L133) versus phosphate-buffered saline (PBS) on days 2 to 6 (asterisks denote  $P < 0.05$ ). (C) Bacteremia of mice immunized with M1 or M1\*( $\Delta$ L133) 4 hours after intraperitoneal challenge with WT M1 GAS. Mean (horizontal bars) and distribution are shown ( $N = 10$  per group). ANOVA was significant at  $P = 0.02$ ; posthoc group comparisons revealed significant protection of M1 or M1\*( $\Delta$ L133) versus PBS control (asterisks denote  $P < 0.05$ ). (D) Kaplan-Meier survival curve of immunized mice from (C).